JOURNAL OF MATERIALS SCIENCE 24 (1989) 2483–2487

The crystal structure of a quenched Cu-rich β-phase with the composition $Cu_{14.0}In_{16.7}Se_{32}$

W. HÖNLE
Max-Planck-Institut für Festkörperforschung, Stuttgart, Federal Republic of Germany
G. KÜHN, U.-C. BOEHNKE
Sektion Chemie der Karl-Marx-Universität, Leipzig, GDR

The crystal structure of a Cu-rich β-phase in the system Cu–In–Se with the composition $Cu_{14.0}In_{16.7}Se_{32}$ quenched from 750° C, has been determined with single crystals. The investigated single crystal of this Cu-rich β-phase has the composition $Cu_{14}In_{16.7}Se_{32}$ and crystallizes with $a = 1.1534(4)$ nm in the space group $P\bar{4}3m$. The cations are statistically distributed together with vacancies, but show strong preferences for distinct positions. The number of vacancies is estimated from the crystal structure analyses and is found to be much less than in the Cu-poor β-phase. The crystal structure is compared with that of an ordered Cu-rich β-phase.

1. Introduction

Recently, we reported on the crystal structures of two quenched phases of the system Cu–In–Se, namely the δ-phase and a Cu-poor β-phase [1]. The δ-phase crystallizes with the sphalerite type of structure in the space group $F\bar{4}3m$, whereas the β-phase represents a new chalcopyrite type in the space group $P\bar{4}2c$. Both structures are characterized by nearly fully occupied anion sites, whereas the cation sites are filled by Cu, In and vacancies. There is already a crystal structure determination reported of the ordered cubic Cu-rich β-phase [2]. Now we report on the crystal structure of a quenched Cu-rich β-phase.

2. Synthesis and characterization

2.1. Synthesis

The synthesis of the Cu-rich β-phase has been performed in the course of an investigation of the quasibinary section Cu_2Se/In_2Se_3. Samples of this phase have been synthesized by melting mixtures of the elements (5N purity) at 1370 K, annealing 20 days at 1020 K and quenched with H_2O to room temperature [3].

2.2. Chemical analyses

The chemical analyses were performed with selected single phased samples via ESMA, calibrated by combined wet chemical analysis (gravimetric/coulometric) [3] as well as after the digestion in the modified teflon liner [4] by ICP analyses, see Table I.

2.3. X-ray powder photographs

The X-ray powder photographs have been recorded with the Guinier method (ENRAF-NONIUS, Delft; flat sample) as well as with the powder diffractometer HZG 4 (Präzisionsmechanik Freiberg/Sachsen). The determination of the lattice constants has been calibrated with silicon.

TABLE I Chemical analysis

Phase	Element	Composition (at %) by		Average composition
		ESMA	ICP	
β	Cu	15.2	16.8	
Cu-rich	In	31.0	31.3	$Cu_{0.61}In_{1.18}Se_{2.00}$
	Se	53.8	51.8	

The compositions resulting from the chemical analyses have been normalized to Se = 2.0 as well as to electroneutrality.

2.4. X-ray structure determination

The crystal was broken of a specimen with the composition of the bulk being $Cu_{9.7}In_{18.9}Se_{32}$, as revealed by ESMA and ICP analyses. The crystal was mounted into a glass capillary and checked with precession

TABLE II Crystallographic data and details of the structure determination

Formula	$Cu_{14.0}In_{16.7}Se_{32}$
Lattice constants of refined 2θ-values of 12 *h k l* at 295 K	$a = 1.1543(4)$ nm
Space group (no.); Z	$P\bar{4}3m$ (215); 1
Intensity measurement	automated four circle diffractometer; SYNTEX R$\bar{3}$, graphite monochrom.; scintillation counter, Mo$K\alpha$($\lambda = 0.71073$ nm); $2\theta \leqslant 60°$; variable scan rate; ψ-scan absorption correction.
Refinement	Program system SHELXTL [5]; full matrix least squares
$N(hkl)$; $N'(hkl)$ with $F \geqslant 3\sigma(F)$	1922; 379
N (parameter)	44
R (aniso); R (w)	0.046; 0.049

Further details of the crystal structure determination are deposited at the Fachinformationszentrum Energie, Physik, Mathemathik GmbH, D-7514 Eggenstein-Leopoldshafen 2 and are available on quoting CSD 53018, the names of the authors and the journal reference.

TABLE III Positional parameters and temperature factor coefficients (standard deviation) ($U_{ij} \times 10^{-6} T_2 nm^2$). The atomic label behind the positions M give the atomic scattering factor used at this positions (Cu or In), valid for the refinement only

Atom	Site	x	y	z	U_{eq}	U_{11}	U_{22}	U_{33}	U_{12}	U_{13}	U_{23}	SOF
Se1	4e	0.8862(6)	x	x	130(18)	130(32)	U_{11}	U_{11}	−28(25)	U_{12}	U_{12}	1
Se2	4e	0.3722(6)	x	x	382(20)	382(34)	U_{11}	U_{11}	26(39)	U_{12}	U_{12}	1
Se3	12i	0.1207(6)	x	0.3856(5)	192(15)	222(26)	U_{11}	133(26)	50(26)	−19(18)	U_{13}	1
Se4	12i	0.3781(4)	x	0.8707(6)	162(12)	171(21)	U_{11}	143(19)	−76(24)	20(20)	U_{13}	1
M1(In)	1b	1/2	1/2	1/2	517(37)	517(64)	U_{11}	U_{11}	0	0	0	0.912(24)
M2(In)	3c	1/2	1/2	0	517(37)	501(92)	330(72)	U_{22}	0	0	0	0.680(16)
M3(In)	12i	0.2500(1)	x	0.0011(9)	278(4)	295(7)	U_{11}	246(7)	21(37)	3(16)	U_{13}	1
M4(In)	12i	0.2498(3)	x	0.500(2)	513(9)	505(15)	U_{11}	528(15)	−155(58)	−12(32)	U_{13}	0.690(6)
M5(Cu)	3d	0	0	1/2	1122(117)	1115(245)	1125(178)	U_{22}	0	0	0	0.816(24)

The U_{ij} are defined for $\exp[-2\pi^2(U_{11}h^2a^{*2} + \cdots + 2U_{23}hka^*b^*)]$

photographs. It was found to consist of a main domain and a small parasitic phase, visible in one photograph only. The size of this parasitic phase was estimated to be less than 3 vol %. The intensity data of the main domain were collected on an automated four-circle diffractometer. Further crystallographic details of the data collection and refinement are summarized in Table II. Table III gives the positional parameters, Table IV bond distances and angles.

The cation positions are labelled by M1 to M4. As analogous to the procedure given in [1], we also vary the site occupancy factors (SOF) as well as the type of scattering factors of the cations (for the calculation of the occupancy of Cu and In at the cation positions see below). The anion positions were found to be occupied with SOF = 1 within standard deviations. Checks for anomal dispersion effects were performed, manifesting the model given in Table III.

A refinement in space group $P23$ yields the same R factors, the positions being the same as those in Table III for the higher symmetric space group. During the refinement we also checked the crystal structure of the ordered β-phase, as given by [2]. The refinements with their model, but our data, failed with $R \sim 25\%$.

The interpretation of the refined occupancy factors with respect to the cation and vacancy distribution follows the same lines as given in [1].

3. Results and discussion

Table II gives the lattice constant and details of the structure determination, Table III the positional and thermal parameters and Table IV the bond distances

TABLE IV (a) Bond distances in nm and (b) bond angles in degrees

(a) Site	Bond distance ($\times 10^{-3}$ nm)	Multiplicity
Se1-M3	258.9(9)	3x
Se2-M4	248(2)	3x
-M1	255.5(7)	
Se3-M5	237.2(7)	
-M4	249(1)	
-M3	256.6(9)	2x
Se4-M4	247(1)	2x
-M2	248.7(6)	
-M3	257.7(8)	
M1-Se2	255.5(7)	4x
M2-Se4	248.7(6)	4x
M3-Se3	256.6(9)	2x
-Se4	257.7(8)	
-Se1	258.9(9)	
M4-Se4	247(1)	2x
-Se2	248(2)	
-Se3	249(1)	
M5-Se3	237.2(7)	4x

(b) Site	Bond angles (deg.) (SD)	Multiplicity
Se1		
M3-M3	104.7(3)	3x
Se2		
M4-M4	110.6(5)	3x
M4-M1	108.3(5)	3x
Se3		
M5-M4	114.1(5)	
M5-M3	111.4(3)	2x
M4-M3	107.3(4)	2x
M3-M3	104.7(3)	
Se4		
M4-M4	111.4(5)	
M4-M2	110.8(5)	2x
M4-M3	108.2(3)	2x
M2-M3	107.4(3)	
M1		
Se2-Se2	109.5(3)	6x
M2		
Se4-Se4	106.3(3)	2x
Se4-Se4	111.1(2)	4x
M3		
Se3-Se3	114.8(5)	
Se3-Se4	107.3(2)	2x
Se3-Se1	107.0(2)	2x
Se4-Se1	113.4(4)	
M4		
Se4-Se4	110.5(9)	
Se4-Se2	108.5(2)	2x
Se4-Se3	108.9(3)	2x
Se2-Se3	111.5(9)	
M5		
Se3-Se3	112.3(3)	2x
Se3-Se3	108.1(3)	4x

TABLE V Site distribution

Site	Cu	In	□
M1	–	0.91	0.09
M2	1.71	1.29	–
M3	–	12.00	–
M4	8.16	3.84	–
M5	2.45	–	0.55

TABLE VI Idealized positions of the Cu-rich β-phase (top) and $Cu_{8.5}In_{18.5}Se_{32}$ [2]·(bottom). Majuscules denote anions, miniscules denote cations

Lable	Occupancy	Site	x	y	z
a	M1	1*b*	1/2	1/2	1/2
b	M2	3*c*	1/2	1/2	0
c	M3	12*i*	1/4	1/4	0
d	M4	12*i*	1/4	1/4	1/2
e	M5	3*d*	0	0	1/2
f	□	1*a*	0	0	0
A	Se1	4*e*	7/8	7/8	7/8
B	Se2	4*e*	3/8	3/8	3/8
C	Se3	12*i*	1/8	1/8	3/8
D	Se4	12*i*	3/8	3/8	3/8
a	In	12*h*	1/4	1/2	0
b	In	6*g*	1/4	1/2	1/2
c	Cu	4*e*	1/4	1/4	1/4
d	Cu	4*e*	3/4	3/4	3/4
e	□	6*f*	1/4	0	0
A	Se1	4*e*	1/8	1/8	1/8
B	Se2	4*e*	5/8	5/8	5/8
C	Se3	12*i*	3/8	3/8	1/8
D	Se4	12*i*	1/8	1/8	5/8

and bond angles. The distribution of In and Cu at the positions M1 to M5 is performed in the following way:

For the distance d(Cu–Se) and d(In–Se) one calculates with the values of Pauling's tetrahedral radii $r^{[4]}$ Cu = 0.135, $r^{[4]}$ Se = 0.114 and $r^{[4]}$ In = 0.144 nm with respect of the polarity correction by Schomaker and Stevenson values of d_1(Cu–Se) = 0.2450 nm and d_1(In–Se) = 0.2535 nm. A simple linearic interpolation for the observed ratio (34% Cu, 66% In) yields a value of d_c(In/Cu–Se) = 0.2506 nm for a distance from a $M(Cu_{0.34}In_{0.66})$ position to Se. Having the M positions occupied with Cu or In exclusively, this value may deviate approximately 0.005 nm down (Cu) and up (In), respectively. With those ideal bond distances in mind, the distribution of Cu and In proceeds as follows: M3 with $\bar{d}$(M4–Se) = 0.2575 nm is occupied with In only, the similar holds for M5 with $\bar{d}$(M5–Se) = 0.2372 nm, being occupied with $Cu_{0.816}$. The positions M2 and M4 have nearly the same occupation with Cu and In as indicated by bond distances and SOFs [$\bar{d}$(M2–Se) = 0.2487 nm; $\bar{d}$(M4–Se) = 0.2477 nm]. Position M1 is occupied mainly with In, as indicated by the bond lengths [$\bar{d}$(M1–Se) = 0.2555 nm] and the SOF [$In_{0.91}$]. Thus one obtains the distribution (based on 32Se) given in Table V, yielding after renormalization to electroneutrality the composition $Cu_{11.9}In_{17.4}Se_{32}$. The SOFs of the Se positions do not deviate within standard deviations from unity, therefore they would hold constant. Taking the SOFs of the positions M2 and M4 as a scale for the occupancy, one obtains from the analyses of the atomic scattering power a somewhat higher Cu and somewhat lower In content at these positions, namely $Cu_{14.0}In_{16.7}Se_{32}$.

It turns out, that in comparison to the Cu-poor β-phase a much lower number of vacancies is present in the Cu-rich β-phase.

Figure 1 displays the schematic projections of the quenched as well as of the ordered β-phase [2]. The heights have been given in terms of 1/8 of the axis, for the labelling of the positions cf. Table VI. There are some differences between the two phases: Whereas in the quenched phase there is only one ordered vacancy present (site 1a), the ordered phase contains six vacancies (site 6f). Another remarkable difference is the distribution of cations at five different sites in the quenched and at four sites in the ordered phase. Both phases are equivalent with respect to the anion distribution as well as with the much less number of vacancies with the anion sites.

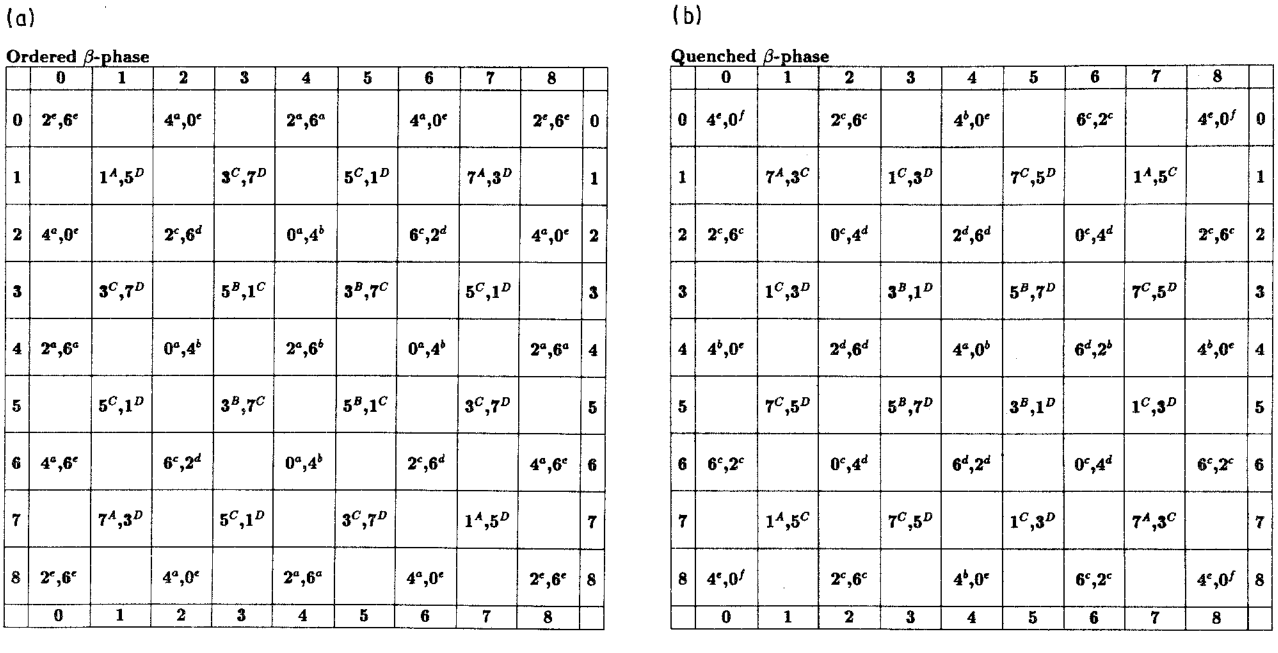
(a)

Ordered β-phase

	0	1	2	3	4	5	6	7	8	
0	$2^e,6^e$		$4^a,0^e$		$2^a,6^a$		$4^a,0^e$		$2^e,6^e$	0
1		$1^A,5^D$		$3^C,7^D$		$5^C,1^D$		$7^A,3^D$		1
2	$4^a,0^e$		$2^c,6^d$		$0^a,4^b$		$6^c,2^d$		$4^a,0^e$	2
3		$3^C,7^D$		$5^B,1^C$		$3^B,7^C$		$5^C,1^D$		3
4	$2^a,6^a$		$0^a,4^b$		$2^a,6^b$		$0^a,4^b$		$2^a,6^a$	4
5		$5^C,1^D$		$3^B,7^C$		$5^B,1^C$		$3^C,7^D$		5
6	$4^a,6^e$		$6^c,2^d$		$0^a,4^b$		$2^c,6^d$		$4^a,6^e$	6
7		$7^A,3^D$		$5^C,1^D$		$3^C,7^D$		$1^A,5^D$		7
8	$2^e,6^e$		$4^a,0^e$		$2^a,6^a$		$4^a,0^e$		$2^e,6^e$	8
	0	1	2	3	4	5	6	7	8	

(b)

Quenched β-phase

	0	1	2	3	4	5	6	7	8	
0	$4^e,0^f$		$2^c,6^c$		$4^b,0^e$		$6^c,2^c$		$4^e,0^f$	0
1		$7^A,3^C$		$1^C,3^D$		$7^C,5^D$		$1^A,5^C$		1
2	$2^c,6^c$		$0^c,4^d$		$2^d,6^d$		$0^c,4^d$		$2^c,6^c$	2
3		$1^C,3^D$		$3^B,1^D$		$5^B,7^D$		$7^C,5^D$		3
4	$4^b,0^e$		$2^d,6^d$		$4^a,0^b$		$6^d,2^b$		$4^b,0^e$	4
5		$7^C,5^D$		$5^B,7^D$		$3^B,1^D$		$1^C,3^D$		5
6	$6^c,2^c$		$0^c,4^d$		$6^d,2^d$		$0^c,4^d$		$6^c,2^c$	6
7		$1^A,5^C$		$7^C,5^D$		$1^C,3^D$		$7^A,3^C$		7
8	$4^e,0^f$		$2^c,6^c$		$4^b,0^e$		$6^c,2^c$		$4^e,0^f$	8
	0	1	2	3	4	5	6	7	8	

Figure 1 Schematic drawing of the (a) ordered and (b) quenched β-phases. For the labels cf. Table VI, the heights are given in units of 1/8. Majuscule denote anions (A–D), miniscule denote cations (a–f).

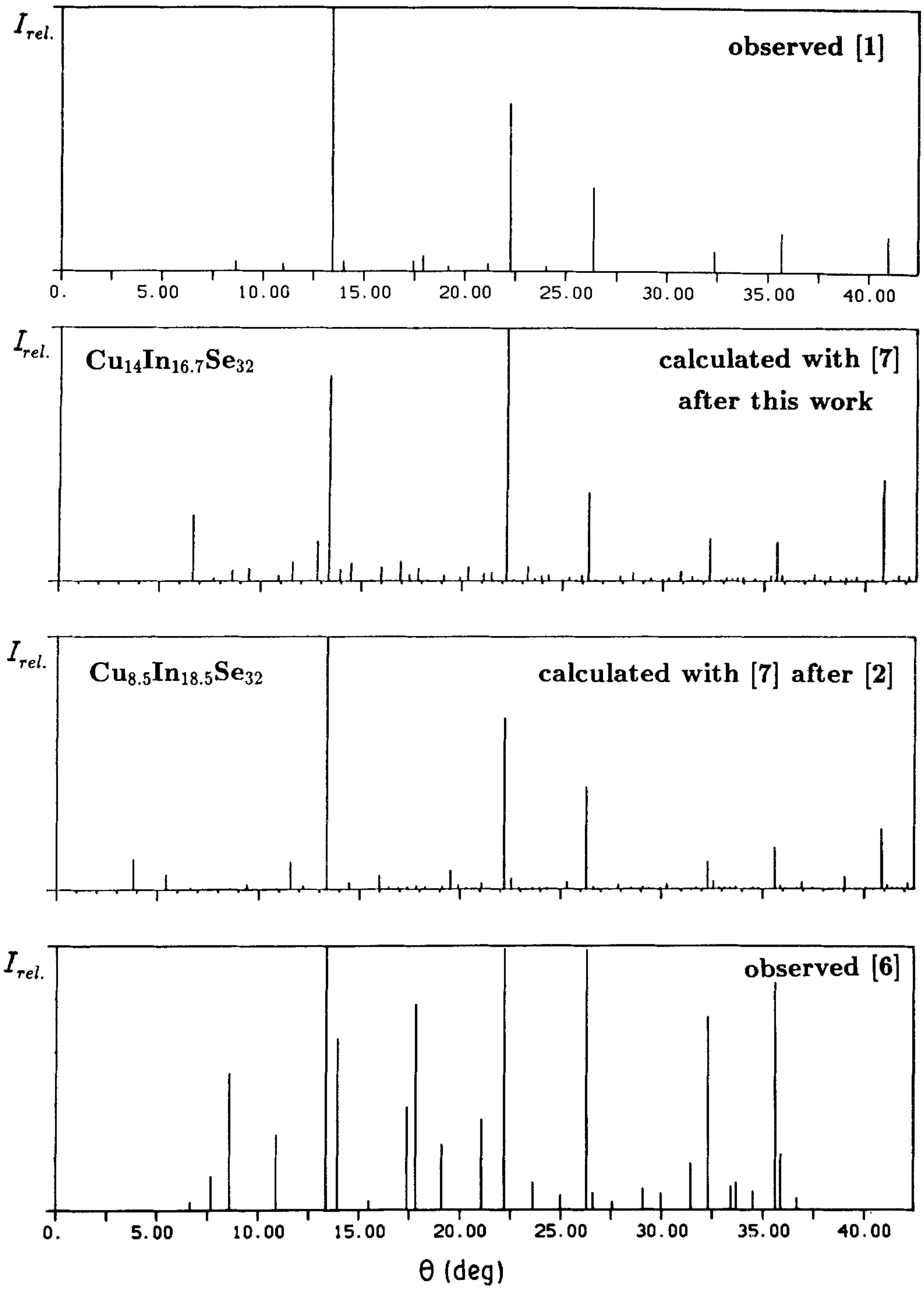

Figure 2 Calculated (with [7], Guinier geometry, $\lambda CuK\alpha 1 = 0.154\,056$ pm) and observed powder diagrams for the quenched (top) and ordered (bottom) β-phase. The data used are those of Tables II and III (this work) and those of references [2, 6]. For purposes of comparison the same lattice constants have been used for the calculation.

Figure 2 gives the observed powder patterns as well as those calculated from the single crystal structure analyses for the quenched and the low-temperature β-phase, as being reported by [6]. In both cases there is no agreement between the calculated [7] and the observed powder patterns. This means, that the single crystals, isolated and investigated in this work as well as in the former [2, 6] work, is not a representative specimen. Another explanation might be the occurrence of tribochemistry, destroying the cubic phases and resulting in phases with higher disorder.

Acknowledgements

We thank Dr K. Peters and Mrs O. Buresch (both MPI, Stuttgart) for measurements of the intensities and the ICP analyses and Dr B. Schumann (KMU Leipzig) for valuable discussions.

References

1. W. HÖNLE, G. KÜHN and U.-C. BOEHNKE, *Cryst. Res. Technol.* **23** (1988) 1347.
2. C. DJEGA-MARIADASSOU, A. RIMSKY, R. LESUEUR and H. J. ALBANY, *Jpn J. Appl. Phys., Suppl.* **19** (1980) 89.
3. U.-C. BOEHNKE and G. KÜHN, *J. Mater. Sci.* **22** (1987) 1635.
4. O. BURESCH and H. G. VON SCHNERING, *Fresenius Z. Anal. Chem.* **319** (1984) 418.
5. G. M. SHELDRICK, SHELXTL, A Program System for

Crystal Structure Determination, Cambridge, unpublished (1978).

6. R. LESUEUR, C. DJEGA-MARIADASSOU, P. CHARPIN and J. H. ALBANY, *Inst. Phys. Conf. Ser.* **35** (1977) 15.

7. K. YVON, W. JEITSCHKO and E. PARTHÉ, *J. Appl. Crystallogr.* **10** (1977) 73.

Received 4 May
and accepted 9 September 1988